Compositional ordering in SiGe alloy thin films

K. L. Whiteaker* and I. K. Robinson
Department of Physics, University of Illinois at Urbana-Champaign, 1110 West Green Street, Urbana, Illinois 61801

J. E. Van Nostrand† and D. G. Cahill
Department of Material Science and Engineering and Materials Research Laboratory, University of Illinois at Urbana-Champaign, 1101 West Springfield Street, Urbana, Illinois 61801

(Received 24 November 1997)

We have performed surface x-ray diffraction experiments on $Si_{0.5}Ge_{0.5}$ films grown on Ge(001) substrates. The results for our thinnest film (eight monolayers) show the compositional order at the initial stages of growth. This ordering is observed underneath the surface (2×1) dimer reconstruction, and was previously predicted by calculations on the equilibrium alloy surface. This initial surface compositional ordering is also consistent with the ultimate structure for the bulk of these films. Measurements from thicker alloy films show an increase in the average order parameter with increasing thickness, but then a decrease with the thickest film of 1000 Å. [S0163-1829(98)03319-0]

I. INTRODUCTION

The silicon germanium alloy is an important example of a semiconductor alloy, and understanding its phenomena is increasingly valuable as alloys become used in electronic devices today. Part of that understanding is the material's atomic crystal structure, which is then the basis for understanding other properties, such as the electronic band structure, defects, and surface growth morphologies. Molecular beam epitaxy (MBE) is an important technique for the growth of novel thin film materials and structures. With the MBE growth technique there is an interface between the environment of incoming species for growth and the growing crystal film. The interface is not in thermal equilibrium, but is instead a driven system, driven by the growth process. The resulting film material and its structure depend on a number of growth conditions. The substrate temperature, film thickness, vicinal (miscut angle), and flux are examples of parameters that affect the resulting crystal film. Another important condition is the structure of the growing interface. The interface can have reconstructions of surface atoms that can then affect the crystal film growth. Silicon and germanium (001) surfaces, including their alloy, have the dimer 2×1 reconstruction. This reconstruction is believed to cause the growth of compositionally ordered films of SiGe(001).

SiGe alloy films were at first assumed to be the same as the bulk solid, a completely random solid solution of both elements with the diamond structure. Then Ourmazd and Bean[1] among others[2,3] found additional Bragg peaks in electron diffraction patterns of alloy layers within Si_xGe_{1-x}/Si(001) superlattices. Pictures of transmission electron diffraction (TED) patterns showed additional peaks at $(\frac{1}{2},\frac{1}{2},\frac{1}{2})$ positions, meaning that there is some structure with double the bulk's cubic periodicity along the $\langle111\rangle$ directions. These weak superstructure peaks are due to compositional correlations of the SiGe alloy. This correlation (or ordering) of Si and Ge atoms on the diamond lattice sites has gained considerable attention, since it could affect the electronic band structure and the material's adjustable band gap is of technological importance. Our x-ray diffraction experiments to investigate the structural ordering of SiGe is the main focus of this paper.

A. The bulk and thermodynamics

To understand the solids formed by the combination of silicon and germanium, as well as other group IV elements, one must look at the bulk thermodynamics. That is, the free energy difference between proposed ordered or disordered structures and the separate elements (phase separation) needs to be calculated. This energy difference can be written as

$$\Delta H = E_{\mathrm{VD}}(a_0) + E_{\mathrm{elect}}(\alpha) + E_{\mathrm{relax}}(\alpha) - T\sigma. \qquad (1)$$

The first term describes the *volume deformation* energy needed to first expand and then contract the diamond lattices for the smaller and larger species, respectively, for the binary compound with lattice spacing a_0. This elastic term is always positive because both elemental solids are deformed from equilibrium. With C/Ge and Ge/Sn, this term, and a possible positive second term, cannot be overcome and results in phase separation for these compounds. The second term is the *electronic* energy, which can include the formation of chemical bonds and the band structure. This term can be negative, as with SiC, which forms chemical bonds, or it can be positive. Martins and Zunger have calculated such a small positive bonding energy for Si and Ge.[4] The third term describes the local elastic *relaxations*, which depend on the ordering α, with the diamond lattice. Certain ordered structures can have large relaxation of the bonds between the different species. An example is the zinc blende structure and its familiar form in GaAs. This cubic structure also occurs for SiC and has been calculated to its lowest energy phase.[4,5] For SiGe, no bulk ordered phases have been observed.[5] The relaxation energy is also important in disordered solids, but it will be higher than a long range ordered solid because of statistical deviations from the average composition and structure. The last term in the energy difference equation is entropy, σ. The negative entropy term is the main reason for

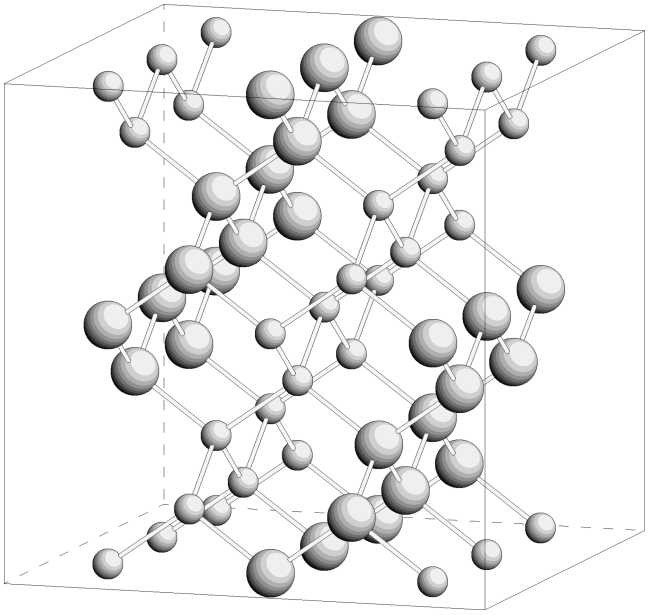

FIG. 1. The bilayer rhombohedral structure (RS2) for the compositional ordering of $Si_{0.5}Ge_{0.5}(001)$ epitaxial thin films. The larger and smaller spheres represent sites of higher Ge and Si compositions, respectively.

the existence of the bulk solid solution formed for alloys of Si and Ge. The magnitude of σ relative to the E terms of Eq. (1) establishes the existence of a ''disordering'' critical temperature above which this solid solution state is preferred.

For SiGe the small chemical bonding contribution leaves the elastic arguments to predict a structure. This leads to two structures: the zinc blende and the rhombohedral (labeled RS1).[4] In both, the structural degrees of freedom allow them to be intrinsically strain free. All bonds are exactly at tetrahedral angles and the bond lengths can be any value. While the zinc blende is an fcc ordered structure, the RS1 has alternating Si/Ge within the (111) double layers denoted by (. . . SiGe-GeSi-SiGe . . .). This was the structure proposed initially to explain the observed superstructure peaks in the TED patterns[1] and was demonstrated theoretically[6] to be the most stable structure in the presence of uniaxial strain. Although the RS1 structure has ordering in only one [111] direction, the (001) surface has four equivalent $\langle 111 \rangle$ directions and so four rotational domains are also proposed to explain all the observed $(\frac{1}{2},\frac{1}{2},\frac{1}{2})$ peaks. As promising as RS1 may be, calculations indicate that the disorder-order transition for this structure, implicit in Eq. (1), occurs well below the temperatures necessary for bulk diffusion, and therefore it is kinetically unachievable.[4,7] This agrees with what is found for bulk SiGe, where annealing for long periods has not achieved any ordered structures.[5]

B. Compositional ordered structures

Other structures that are consistent with the electron diffraction images are discussed next. Another rhombohedral structure (labeled RS2) has the opposite ordering within the (111) double layers, with a sequence of . . . SiSi-GeGe-SiSi-GeGe . . . , and is shown in Fig. 1. Because it necessarily introduces strain in the bond angles, this structure is energetically less favorable than RS1, by as much as 10 meV per atom.[6] However, the RS2 structure is supported by one of the proposed mechanisms to be discussed below. Another possible structure considered is a generalized rhombohedral structure (labeled RS3) that is parametrized to be a range of structures between RS1 and RS2.[8] Each of the four (111) layers has a parameter for the probability of composition. This structure's proposed mechanism will be discussed.

Although all these structures are consistent with the diffraction symmetry for ordered Si_xGe_{1-x} films, only RS2 (and RS3 with parameters close to RS2) is consistent with the *ex situ* x-ray structure factors. The experiment by Tischler *et al.*[9] on a 2800 Å thick MBE $Si_{0.5}Ge_{0.5}$ film on Si(001) provided the quantitative crystallographic analysis to differentiate among the proposed structures. This provides the best evidence for the bilayer ordering of the RS2 structure, shown in Fig. 1. For this sample, the degree of ordering was found to be only 14%, while other groups have reported ordering parameters as high as 0.60.[10] According to the arguments above, only the RS1 structure is thermodynamically stable, so different origins for the compositional ordering in SiGe need to be explored next, to explain why it is the metastable structure that is observed.

C. Growth surface and conditions

Since bulk equilibrium thermodynamics do not agree with the observed Si_xGe_{1-x} film structure, kinetic processes must be considered. The MBE growth surface is clearly the place where kinetics are expected to enter, as this surface at typical growth temperatures is far from equilibrium. A number of experiments have indeed shown the surface to be important. First, the growth conditions under which the ordered structure occurs is only on (001) substrates and always with lower than usual growth temperature (below 550 °C).[1–3,11,9,10,12] Films on (111) substrates are found to be random solid solutions. Second, annealing the (001) ordered films to over 650 °C causes an irreversible transition to the disordered (or random) structure.[13] Others report the needed temperature is 800 °C.[14] In our experiments a temperature of 700 °C was needed before the $Si_{0.5}Ge_{0.5}$ films started to become disordered. The authors of Ref. 13 also found the transition temperature decreased as the stoichiometry of the films moved away from the 50–50 % composition. They proposed a kinetic ''phase diagram'' of the transition as a function of stoichiometry. Another important detail that was found is the importance of the surface reconstruction on $Si_xGe_{1-x}(001)$ crystal.[13]

The effect of doping or covering the growth surface with surfactant type atoms (Sb) removes the (2×1) surface reconstruction. Introducing this change is also found to destroy the compositional ordering. In a dramatic experiment,[13] a single $Si_{0.5}Ge_{0.5}$ sample was made with the surfactant present during the second half of the growth. Only the first half of the sample showed the ordering peaks by TED. Alongside it, the *in situ* low energy electron diffraction (LEED) experiment showed the corresponding switch of the surface structure during the film growth between the (2×1) and the (1×1). This result for Sb doping has also been seen in some degree for Ga and H (low temperature gas-source MBE).[13]

Epitaxial strain is one growth condition that apparently does not interfere with the ordering. The compositional or-

dering has been observed with growth on Si(001) substrates[11,9,10] and on Ge(001) substrates (our experiments and in Ref. 12). Ordering is also observed in films grown on graded buffer layers that are fully relaxed to provide a substrate with the same lattice parameter as $Si_{0.5}Ge_{0.5}$.[13] The strength of compositional ordering peaks in TED and x-ray diffraction depends on the average composition of the $Si_xGe_{1-x}(001)$ alloy films. In the study by Araki *et al.*, the compositional ordering is a maximum at the 50%–50% alloy composition and decreases symmetrically to both sides of this composition. As expected, this rate of ordering decreases linearly with average alloy composition, to the minimum (no ordering) at either 0 or 100% compositions.

These details of the growth conditions lead to the general conclusion that the SiGe ordering results from metastable, kinetically limited structures that form at the growing surface. Once this surface process occurs, the resulting order becomes frozen into the resulting film in the form of the observed metastable RS2 (and RS3) structure.

D. Proposed mechanisms

To understand the process in forming the $Si_xGe_{1-x}(001)$ ordered structure, a number of theories have been proposed that involve the growth process on the dimer reconstructed surface. We will discuss two proposed mechanisms for the ordering; one by LeGoues *et al.*[13] and the other by Jesson *et al.*[15]

The mechanism proposed by LeGoues *et al.* is based on a direct Monte Carlo simulation of the segregation at the $Si_{0.5}Ge_{0.5}(001)$ 2×1 surface previously carried out by Kelires and Tersoff:[16] Ge segregates to the surface because of its lower free surface chemical energy and drives an oscillation of composition in the alloy within the first four layers below the 2×1 reconstructed surface. This equilibrium structure can be understood in terms of local strain associated with the reconstruction, which is known to cause stresses down to at least six layers below the surface.[17–20] In the layers below the surface of the alloy, Ge and Si atoms tend to migrate to sites of tensile and compressive stress, respectively. This subsurface ordering can be understood using the simple argument that the smaller Si atoms find the ''smaller'' sites (under compression) and the larger Ge atoms find the ''larger'' sites (under tension). The growth ordering mechanism occurs by this local equilibrium forming on 2×1 reconstructed terraces.

Kelires and Tersoff were able to calculate the temperature dependence of this near-surface equilibrium order.[16] The degree of surface ordering decays strongly with temperature, with the maximum (100% order) at $T=0$, and about 15–5 % for the growth temperatures typically used. Based on this, LeGoues *et al.* proposed a model for the film growth, consisting of double-height steps propagating across the surface. The ordering becomes frozen in the sixth and fifth layers, while newer layers order to a 2×1 once again. The stacking sequence for the $\langle 111\rangle$ ordering is maintained by the bilayer steps and the energy cost to forming stacking faults in the compositional ordering.

The other mechanism, proposed by Jesson *et al.*,[8] is a kinetic process that occurs specifically at a double-step kink as it moves across the 2×1 surface, thus growing the crystal film. The model first assumes that the surface is covered by segregated Ge. Then, a Si adatom (in response to the Ge-rich surface) finds the preferred kink site. While this Si atom may exchange with the Ge atom below, both sites have dangling bonds and therefore have no strong driving force for Ge segregation. Next, another Si adatom arriving from the source finds the next preferred site. In this case, the Si and lower Ge do exchange because of the different bonding from the 2×1 dimer. This process has been labeled by Jesson *et al.* as a Ge atom ''pump'' mechanism.[8] Finally, the second layer of the double step grows over this, again with the assumed Ge-rich surface. With growth of the next double step and kink, flowing in the same direction, the stacking sequence is also correct for $\langle 111\rangle$ ordering.

According to this mechanism, the ordering is a kinetic process from the step flow and asymmetrical segregation with the 2×1 reconstruction. If one assigns probabilities to the segregation and Ge pump mechanisms, the model gives probabilities for each of the four sites, and then to the four (111) layers. This is how Jesson *et al.* came to the structure RS3 with four parameters of composition. Their x-ray structure factor analysis (Ref. 9) could determine a 1% relative difference between similar bilayers, i.e., 1% difference to the RS2 structure. Their other evidence for the RS3 structure was the presence of additional Bragg peaks other than the $(\frac{1}{2},\frac{1}{2},\frac{1}{2})$ type, which break the symmetry of the equal composition bilayers of RS2 structure. Yet these peaks are very weak.

To summarize, the ordering mechanism observed in $Si_xGe_{1-x}(001)$ films is clearly not related to bulk thermodynamics, but to the surface properties during growth. Two mechanisms have been proposed for the residual compositional ordering, but both are based, so far, on indirect evidence. In the rest of this paper, we will present our experiments designed to look for direct evidence of compositional ordering at the surface. Here, the use of surface x-ray diffraction is the ideal tool for examination of compositional ordering in $Si_xGe_{1-x}(001)$. The kinematic scattering allows simple analysis of the data and the penetration of x rays gives structural information beyond the first or second surface layers. X-ray diffraction has proven to be the best tool in determining bulk-ordered metal alloy structures[21] and recent x-ray diffraction experiments have extended the technique to alloy surfaces as well.[22]

This paper is organized into three sections. The first section provides a description of the experiments for the sample MBE growth and x-ray diffraction measurements. The second section provides the results, organized by (i) the results for pure Ge(001) (2×1) reconstruction, (ii) the thinnest (8 ML) $Si_{0.5}Ge_{0.5}$ data and resulting model, (iii) the Fourier difference map result of the same film, and (iv) result of varying film thicknesses and growth temperatures. The final section states the conclusions and some discussion of these results.

II. EXPERIMENT

The observed compositional order in $Si_xGe_{1-x}(001)$ alloys has been clearly connected to the (2×1) reconstruction of the growing interface. For both Si and Ge (001) (2×1) surfaces, the structure has been accurately determined by

surface x-ray diffraction.[17,19] The experiment we have performed is a generalization of this, designed to observe directly the ordering within the reconstruction. A review of this technique is in Ref. 23, but the basic idea is to measure the two-dimensional scattering from the periodicity of the surface or truncation of the bulk crystal. Unlike bulk diffraction, in 2D diffraction one of the three Laue conditions is relaxed, making the diffraction intensity continuous and perpendicular to the surface (called rods). A surface reconstruction has different periodicity than the bulk and so reconstruction rods are separated from the bulk crystal truncation rods. This allows one to measure an intensity coming only from the surface if it has a reconstruction. The intensity along the various rods is measured and then compared with the model of the surface structure, based on the kinematical diffraction theory.

A. Sample growth

The samples of Si_xGe_{1-x} thin films were grown on Ge(001) substrates. The substrates were cleaned and prepared by rinsing and sonication with ultrapure water to dissolve the native oxide and contaminants, then placed in an ultraviolet lamp box for ozone exposure.[24] The ozone is for the rapid regrowth of the germanium oxide and is believed to oxidize any organic contaminants and, combined with the UV radiation, volatilizes the contaminants for removal from the surface. This process of ultrapure water and UV/ozone exposure was repeated several times with the last step being the UV/ozone, performed before the substrate was indium-bonded to a molybdenum sample holder. The sample was then immediately introduced into the vacuum system through a loading vacuum-interlock chamber. After pumping down, the substrate and sample holder were transferred into the growth chamber. The epitaxial growth chamber was a Perkin-Elmer 425 equipped with a dual electron-beam evaporation system containing Si and Ge sources, with a base pressure of 6×10^{-11} Torr. Once inside the MBE chamber, the sample was slowly heated to desorb any remaining gases. The substrate temperature was increased while the chamber pressure was maintained below 5×10^{-10} Torr. At about 450 °C the oxide was removed by thermal desorption, which was confirmed by reflection high-energy electron diffraction (RHEED) showing the (2×1) pattern for the pure reconstructed surface of Ge(001). The final preparation step was the homoepitaxial growth of a germanium buffer layer, usually 1000 Å thick at a deposition rate of 1 Å/s and a substrate temperature of 370 °C.[25,26]

The deposition rate from both of the electron-beam evaporation sources was controlled by active feedback obtained from an electron ionization emission Spectroscopy (EIES) flux monitor. The total deposition thickness was also monitored by a quartz crystal oscillator. This and the EIES monitor are part of the Inficon Sentinel III deposition controller. For the growth of the $Si_{0.5}Ge_{0.5}$ alloy layers, the EIES monitor allows one to actively control the Si and Ge fluxes individually, to maintain the desired composition of 50%–50%. The final composition of the films was later confirmed by Rutherford backscattering spectroscopy (RBS), which showed a slightly Si rich stoichiometry: 57%–43%. The individual element deposition rates where also confirmed by *ex situ* profilometry on edges of test films, both 1.0 ± 0.3 μm thick. Later, one measurement of the alloy film thickness by x-ray reflectivity found a larger than nominal growth thickness by 20%, consistent with the possible Si rich stoichiometry.[32] In this paper, we will continue to refer to the films as the nominal 50%–50% alloy.

B. X-ray diffraction measurements

Once the sample thin film was prepared, it was then transferred through an ultrahigh vacuum transport tube from the MBE chamber to the x-ray chamber for the scattering measurements. The base pressure of this analysis chamber was 3×10^{-10} Torr, which allowed the measurement to last beyond 48 h before the sample surface became contaminated. Contamination was characterized by a decrease in the scattering intensity from the (2×1) surface. One sample was later transferred to another analysis chamber for x-ray photoemission spectroscopy (XPS), which confirmed the minor surface contamination by carbon and oxygen.

The x-ray source was a Rigaku 18 kW copper rotating anode generator with a highly oriented pyrolytic graphite (HOPG) curved crystal to select the Cu $K\alpha$ radiation ($\lambda = 1.54$ Å). The curvature of the monochromator focused the x rays to a 1×1 mm point at the sample position within the UHV chamber. More details of this x-ray analysis chamber are presented in Ref. 27. Vertical slits were used to control the monochromator's focusing. Horizontal slits placed halfway to the sample defined and collimated the incident x-ray beam. The spectral lines α_1 and α_2 were not resolved. This system provided a large flux of x rays at the expense of resolution. The beam divergence from the HOPG monochromator, perpendicular to the focusing direction, was 0.30°. The detector was placed 630 mm from the sample (center of rotation). At half that distance was a Soller slit box, which collimated the diffracted beam in the direction perpendicular to the focusing direction (i.e., in the horizontal scattering plane). The final optical elements were vertical and horizontal slits in front of the detector for definition of the exit beam size and/or view of the sample.

First, the sample was aligned by finding and centering on the Bragg diffraction peaks of the substrate. Then the diffraction intensity of the (2×1) rods was measured for each of the samples. Figure 2 is a picture of reciprocal space along the $\langle110\rangle$ plane, showing the relative locations of diffraction intensity from the sample. The dark circles represent the bulk Bragg peaks from the substrate and the SiGe thin film, with the open circles showing the missing fcc type peaks. The crystal truncation rods are the continuous intensity lines shown between the bulk peaks. The long range ordered domains within the SiGe films are represented by the gray circles, the first being half the distance to the (111) bulk peak. The superstructure peaks shown represent the superimposed diffraction from all the domains of the ordering. The surface reconstruction rods, represented by the lines between, also run through the ordering peaks. The dimers and their double periodicity give rise to the surface rods, halfway between the bulk crystal truncation rods. The doubling period of the ordering in the (111) bilayers makes the surface rods overlap the ordering peaks.

The experiments measured the intensity only along the surface reconstruction rods, allowing us to be sensitive only

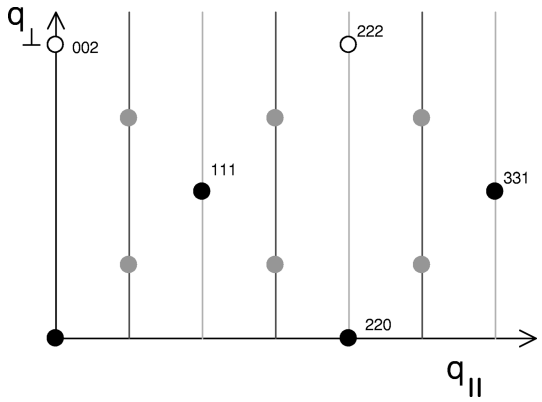

FIG. 2. Sketch of reciprocal space [110] plane for Si_xGe_{1-x} (001) thin film. The solid circles are bulk Bragg peaks and have crystal truncation rods running between them. The grey solid circles are the ordering peaks with reconstruction rods passing through them.

to the surface and ordering structures. For each point along the rod, a θ scan was performed that makes a cross section of the rod giving the integrated intensity.[28] Each θ scan was integrated numerically and background-subtracted, then normalized using an area correction and Lorentz and polarization factors to yield a single structure factor value.[27] The length of the rods measurable was slightly less than that shown in Fig. 2, up to about $L=1.9$, limited by the angular range of the instrument.

We use the common cubic indices, hkl, to describe the reflections from silicon or germanium crystals and surface indices, HKL, to describe the surface diffraction in this experiment. The transformation between them is

$$\begin{pmatrix} H \\ K \\ L \end{pmatrix} = \begin{pmatrix} \frac{1}{2} & \frac{1}{2} & 0 \\ -\frac{1}{2} & \frac{1}{2} & 0 \\ 0 & 0 & 1 \end{pmatrix} \begin{pmatrix} h \\ k \\ l \end{pmatrix}. \tag{2}$$

This surface coordinate frame was chosen so the momentum transfer perpendicular to the surface is along one of the principal axes, L. Using this, the reflections (004), (111), and $(\bar{1},1,1)$ become in surface notation (004), (101), and (011), respectively. For the dimer (2×1) reconstruction, the surface unit cell is doubled along one in-plane direction. Correspondingly, the reciprocal space index becomes a multiple of half integers in that direction. So, the reconstruction rods appear at $(\frac{1}{2},0,L)$, $(\frac{3}{2},0,L)$, $(\frac{1}{2},1,L)$, etc.

The presence of the reconstruction also means the (001) surface breaks its fourfold rotational symmetry. Yet, because the surface is equally covered by two domains of the reconstruction oriented 90° apart, the reconstruction rods occur in the half-order positions both along the surface H and K directions. In the data reduction, the diffraction rods from both domains are combined together to make one data set. The measured half-order rods for the various samples were limited to one half quadrant, the smallest asymmetric volume, and to a maximum in-plane momentum transfer of the $(\frac{5}{2},0,L)$ rod. Test positions were measured to confirm that the symmetry and the related intensities were equivalent.

The final detail is the correction for the leakage of second harmonics. The multichannel analyzer output from the scintillation detector was used to correct the imperfect discrimination between the primary scattered x rays and second harmonic x rays. The harmonic counting rate was multiplied by 6×10^{-5} and then subtracted from the fundamental. This correction was found to change only structure factors near and at $L=0.5$ or 1.5 [because $(\frac{1}{2}\frac{1}{2}\frac{1}{2})$ measures also the x rays with double the energy scattered by the (111) reflection]. The correction ranged from 5% for the larger structure factors up to 20% for some of the weakest data points.

III. RESULTS

A. Ge(001) buffer layer surface

The first experiment performed was to measure the x-ray scattering from the pure Ge surface for later comparison with the SiGe film surfaces. As mentioned above, the Ge(001) substrates were initially grown with a 1000 Å buffer layer to obtain a well-ordered (2×1) surface, which provided the starting surface for the subsequent growth of Si_xGe_{1-x} thin films. We first measured one of these bare substrate surfaces to confirm its structure and to establish an intensity benchmark for calibration.

The structure of the Ge(001) (2×1) surface has been determined before by x-ray diffraction by two groups.[17,18] Rossman *et al.*'s experiment[17] was similar to ours, in that they used a rotating anode x-ray source, but the later measurement of Torrelles *et al.*[18] at a synchrotron radiation source provided finer details of the structure, which came mostly from their larger range of perpendicular momentum transfer, L. The results from our *in situ* surface x-ray diffraction experiment on the same Ge(001) surface are plotted in Fig. 3. This figure shows the complete data set: seven reconstruction rods. Each rod is labeled by its H and K indices. Each data point for the measured structure factor results from an integration scan through a cross section of the rod. To sample the continuous rod intensity, the scans were made every $\Delta L=0.1$. The dashed line represents the structure factors calculated for the model by Torrelles *et al.* This model needs only one free parameter to fit the data, which is an overall scaling factor. Torrelles' model fits very well to the data, giving a $\chi^2=1.52$. This confirms not only that the published Ge(001) model is correct, but also that our instrument and data analysis is working properly, which was important because it was the first experiment for our new instrument. A summary of the main structural features of this model and the next is presented in Fig. 4.

An important detail of the model is that the dimer has an asymmetric tilt angle, but both directions of the tilting are included with equal weight in the amplitude scattering. This disordered buckling dimer structure, proposed by Rossman *et al.*,[17] allows one to model the changing dimer angle across the actual surface. This dimer tilting is believed to be dynamic in nature, because at lower temperatures there is a transition to another reconstruction with the same dimers but ordered into a $c(4\times2)$ reconstruction along the tilt directions of the dimer rows.[29] Another important detail of the Ge(001) (2×1) model is the displacement of atoms down to eight layers below the surface dimer. This result shows the

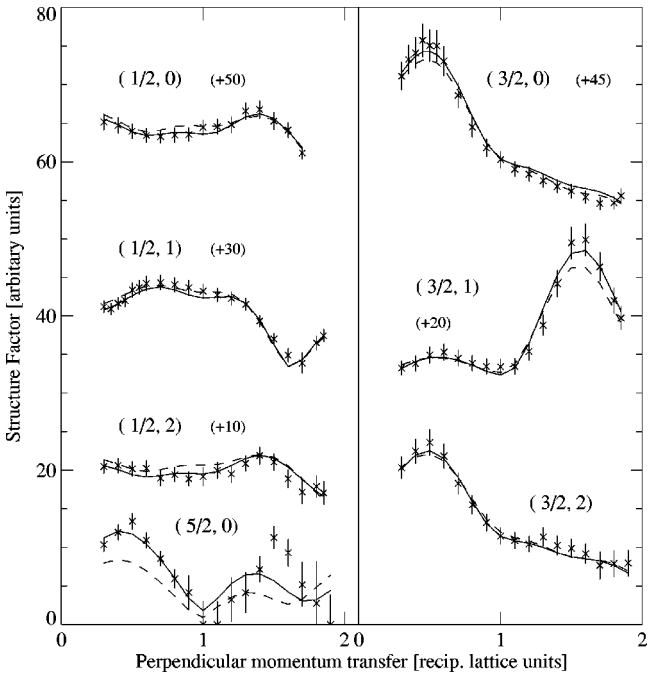

FIG. 3. Measured structure factors versus index L for seven reconstruction rods. The vertical line of each data point represents its uncertainty. The dashed lines are the curves calculated from the model of Torrelles *et al.* The solid lines are curves calculated for our model, fit to these data. For each rod, its H and K indices and vertical offset are indicated.

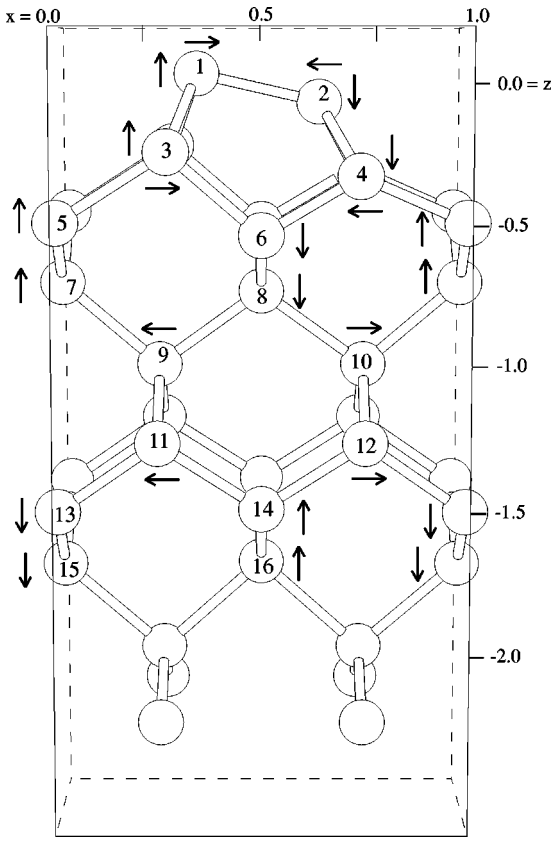

FIG. 4. Structural model of Ge(001) (2×1) reconstruction containing displacements of the atoms from their ideal bulk positions. The directions of the displacements are indicated with arrows. Not shown are the symmetrically equivalent dimer and second layer atoms with the opposite tilt. This structure and its mirror image were combined with equal probability to represent the disordered dimer tilting.

propagation of strain associated with the strong bond bending in forming the dimer reconstruction.

Next, we tried fitting data by adjusting the same displacement and Debye-Waller parameters, starting from Torrelles' parameters. The result is also plotted in Fig. 3 as the solid curves. The new model did decrease χ^2 to 0.61. The structural parameters for our fit are listed in Table I. Our model fits the data closer, especially the peaks in rods $(3/2,0,L)$ and $(3/2,1,L)$, but it gives bond lengths that are slightly farther from the bulk germanium bond length of 2.45 Å. Additionally, with the resulting χ^2 being below 1.0, this could mean our model may be fitting the data beyond its uncertainty, but may also imply a discrepancy in the error estimate of the data. Table II lists the dimer bond length and angle of inclination for our best fit model, the two previous experiments, and other results from Si(001).

B. $Si_{0.5}Ge_{0.5}$(001) very thin film

This section will describe the results for a $Si_{0.5}Ge_{0.5}$ thin film at its initial stage of growth. The film was deposited on a 1000 Å buffer layer at 400 °C with a thickness of only eight monolayers (ML). The sample was transferred after growth to the x-ray chamber for diffraction measurements with exactly the same optical configuration as the Ge(001) experiment. The resulting data set from the very thin film of $Si_{0.5}Ge_{0.5}$ is shown in Fig. 5, which also shows, for comparison as dashed curves, the pure Ge(001) data. The general trend is an overall decrease in the observed structure factors. This is expected because of alloying of some silicon on the surface, the form factor of Si being less than that of Ge because it has fewer electrons. Because of the similarity in the data, we can say that the surface of this thin film still has the dimer reconstruction, but this must now consist of an alloy of Ge and Si atoms. However, the structure is not identical because this would simply reduce the data by a constant scale factor. This is clearly not the result shown in Fig. 5. There are different modulations and additional peaks for some of the rods. The gross features are still present, indicating that the dimers and subsurface displacements are still an important component of the structure. But new peaks occur in addition at or near the positions expected for the alloy (111) bilayer ordering, i.e., at rod positions of $L=\frac{1}{2}$ and $\frac{3}{2}$ as noted by circles in Fig. 2. This cursory inspection suggests that there is some additional order present in the $Si_{0.5}Ge_{0.5}$ thin film, beyond the simple dimer reconstruction.

To quantify the structure, another least-squares refinement was made. The best model with reasonable bond lengths and atomic densities, which fit the structure factors, is shown in Fig. 5. The solid curves calculated from the model matched most of the features of the data and gave $\chi^2=2.1$. Our fit model contained parameters of two types: variable composition at certain lattice positions, and displacements of the near surface atoms. First, the compositions of the dimer and second layer atomic sites were allowed to adopt free values, but both the left and right positions in Fig. 4 were constrained to be the same. These topmost sites were free in composition to model the possibility of Ge segregation. Next, the average

TABLE I. Atomic positions for the best fit model to the Ge(001) 2×1 data set shown in Fig. 3. The coordinates are normalized to the (2×1) unit cell, i.e., $a=8.000$ Å, $b=a/2$, and $c=a_o=5.658$ Å. Asterisks denote fixed coordinates. The numbers in parentheses are calculated uncertainties in the last digit.

Atom	x	y	z	B (Å)
1	0.308(4)	0.5*	0.027(5)	1.9(2)
2	0.633(2)	0.5*	−0.070(6)	
3	0.274(1)	0.0*	−0.245(5)	0.7(5)
4	0.750(1)	0.0*	−0.26(13)	
5	0.0*	0.0*	−0.479(2)	0.50 [a]
6	0.5*	0.0*	−0.517(2)	
7	0.0*	0.5*	−0.732(2)	
8	0.5*	0.5*	−0.760(2)	
9	0.2438(4)	0.5*	−1.00(2)	
10	0.7562(4)	0.5*	−1.00(2)	
11	0.2472(4)	0.0*	−1.25(3)	
12	0.7528(4)	0.0*	−1.25(3)	
13	0.0*	0.0*	−1.503(2)	
14	0.5*	0.0*	−1.491(2)	
15	0.0*	0.5*	−1.754(2)	
16	0.5*	0.5*	−1.747(2)	

[a]Fixed to known bulk factor.

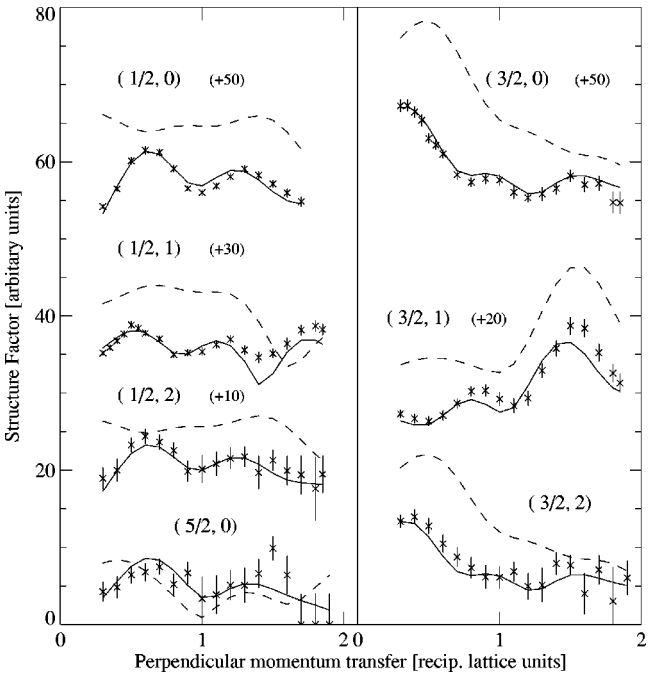

FIG. 5. Measured structure factors versus index L for a $Si_{0.5}Ge_{0.5}$ 8 ML film. The dashed curves are structure factors from Ge(001) for comparison. The solid curves are calculated from our model for the compositional order.

composition within each of the layers 3 through 8 was constrained to the average composition from the growth condition, i.e., the bulk film composition. Since each layer of $Si_{0.5}Ge_{0.5}$ within the unit cell has only two nonequivalent atoms, the composition is then distributed between these two positions, represented by a layerwise order parameter, p. The definition of p is such that when $p=0$, both positions will have the bulk composition. If $p=1$ or -1, then one lattice position has only Si and the other only Ge, meaning the layer is completely ordered. The sign definition is relative to a specific choice of site within the 2×1 unit cell. For the values between these two extremes, p is linearly related to the probability of finding a Ge atom on that site. This definition is similar to that used by Kelires and Tersoff.[16]

Another constraint placed on the model is that the bilayers (layers 3 and 4 and layers 7 and 8) each have the same order parameter. This ordering of bilayers is predicted from the bulk ordering structure RS2 (Fig. 1) determined by Tischler *et al.*[9] In layers 5 and 6, the lateral ordering within each layer cannot be resolved, just as in the case for the dimers above. A vertical mirror plane through the center of the unit cell is assumed from the symmetry of the data set. Therefore, the atoms within each of these layers were constrained to the film's average composition. This does not mean these layers do not have any ordering. It means that the measured structure factors combined the scattering from both possible domains of (111) and $(\bar{1}\,\bar{1}1)$, and therefore could not resolve the possible ordering within these layers. This is analogous to the case in earlier experiments on Ge(001) (2×1), which could not resolve between a symmetric dimer model and disordered dimers with asymmetric buckling.[17]

Besides the density parameters, the model also included displacement parameters. Only the atoms in layers 1 and 2, the dimer and second layer atoms, were allowed to move in the x and z directions during the refinement. All other atoms were fixed at the positions from Torrelles' model for the Ge(001) (2×1) structure. These few displacement parameters helped limit the results to the most meaningful model. The result of the refinement with this model is shown in Fig. 6. The most important conclusion is the ordering in layers 3 and 4 under the dimer and the additional order in layers 7 and 8. The deeper ordering has the correct registry for either the (111) or $(\bar{1}\,\bar{1}1)$ bilayer ordering. This confirms the structure from experiments on thicker and relaxed $Si_{0.5}Ge_{0.5}$ films (described in our measurements below) by Tischler *et al.*[9] The resulting structure also has some Ge segregation: the dimers have a higher germanium composition than the bulk film.

Another result is the increased bond length of the dimers to 2.69 ± 0.15 Å. In general, in the incorporation of Si in the Ge lattice, one expects the average bonds to shorten. Some of the bonds from the dimers to second layer atoms and the bonds from the second to the third layer did shorten. But this dimer bond length is in agreement within uncertainty with other measurements.[20,18]

TABLE II. Ge(001) dimer bond length and angle of inclination from our best fit model and models by others. The last two entries are the same parameters for Si(001) dimer reconstruction for comparison. Bulk bond lengths are 2.35 Å for Si and 2.45 Å for Ge.

Model and Ref.	Bond length	Angle
Our best fit	2.66 ± 0.04 Å	$12\pm3°$
Torrelles *et al.* (Ref. 18)	2.55 ± 0.01 Å	$15.6\pm0.6°$
Rossman *et al.* (Ref. 17)	2.44 ± 0.04 Å	$17\pm4°$
Si(001): Takahashi *et al.* (Ref. 19)	2.37 ± 0.06 Å	$20\pm3°$
Si(001): Felici *et al.* (Ref. 20)	2.67 ± 0.07 Å	$20\pm3°$

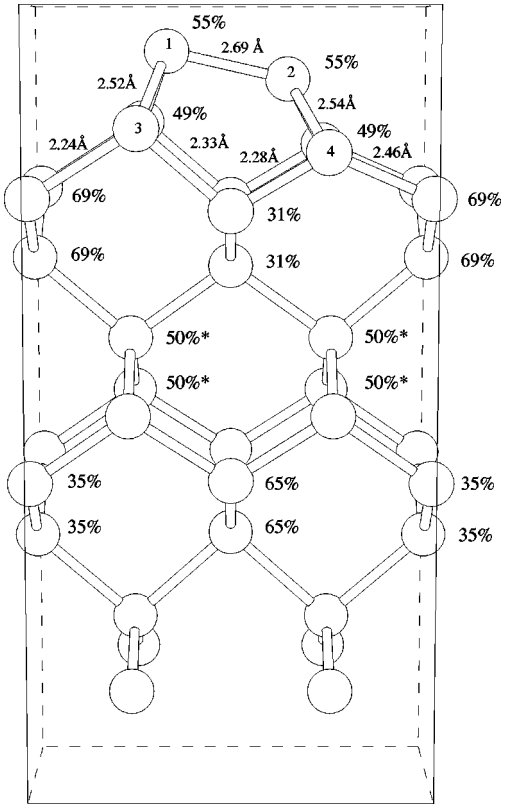

FIG. 6. Resulting model of the $Si_{0.5}Ge_{0.5}(001)$ 8 ML thick film structure. The composition percentages for Ge are listed for each atomic position. The bond lengths shown (in Å) are the only ones determined by the least-squares refinement; all others were fixed to the values of the model of Torrelles for Ge(001). The uncertainties for the compositions of the first and second layer are $\pm 3\%$ and $\pm 5\%$, respectively. The rest have uncertainty of $\pm 1\%$.

Our result agrees with the prediction of Kelires and Tersoff[16] that the Ge compositions in layers 3 and 4 should be 60% at 400 °C (our growth temperature). Their study also predicted a large segregation with a dimer Ge composition of 90%. Our model has some increase in Ge segregation, but not quite this amount. Their equilibrium model also predicted some ordering one layer deeper (7), but only to 53% Ge. The resulting compositional order in layers 7 and 8 is in agreement with the model of LeGoues *et al.* In this model, these deeper layers are ordered as prior surface layers, which are then covered by later deposition.

C. Electron density and difference map

An alternative analysis of the $Si_{0.5}Ge_{0.5}$ thin film data is by the direct method of Fourier difference maps. The goal is to use an inverse Fourier transformation of the structure factors to show directly the difference between the known Ge(001) (2×1) structure and the unknown $Si_{0.5}Ge_{0.5}$ structure as a real space image. The first detail is to construct the electron density map from the Ge(001) structure factors. Besides the amplitude, the inverse Fourier transformation also requires the phase for each data point. The phases can be calculated from a known model, which in this case is the model of Torrelles *et al.* for the Ge(001) (2×1) surface.

The resulting electron density map of the unit cell from the surface rods is not itself a direct picture of the atoms.

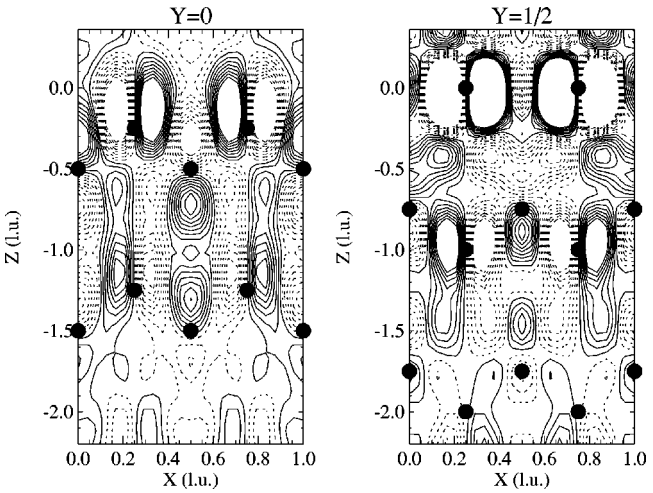

FIG. 7. Electron density map from surface reconstruction structure factors of Ge(001). Map (a) is the $y=0$ plane and map (b) is the $y=\frac{1}{2}$ plane, which includes the dimer atoms. The solid circles mark the ideal bulk positions. Adjacent negative (dashed contours) and positive densities (solid contour) represent the displacement of the Ge atoms from their ideal positions.

Because the crystal truncation rod and Bragg peaks are not included in the inverse transform, only the ''reconstruction density'' is given. This is the difference between the ideal unreconstructed surface and the reconstructed one. By transforming only the odd half-integer rods to the doubled (2×1) surface unit cell, the density pattern is also constrained to have antisymmetric density. As shown in Fig. 7, the density map from Ge(001) has equal negative and positive peaks. In fact, these dipole features show how the Ge atoms move, i.e., from the bulk (symmetric) position to the reconstructed (nonsymmetric) position with the antisymmetric component shown here. The figure shows for the two different y planes the ideal bulk lattice position as solid circles. As expected, the strongest feature is the dimer.

For the $Si_{0.5}Ge_{0.5}$ structure, similarly, the inverse Fourier transformation of only the odd half-index rods will give the antisymmetric density component. This shows where the atoms move from their ideal positions and where the chemical composition is ordered (of interest). But the phases for $Si_{0.5}Ge_{0.5}$ are of some question. We wish to test the model above, and using phases calculated from it may bias the resulting density map. The alternative is to calculate the Fourier difference map between the $Si_{0.5}Ge_{0.5}$ density and the Ge(001) structure for which the phases are known. The difference map is a common method in crystallography to locate missing components in atomic models.[23]

The structure factors and phases from the Ge(001) dimer structure were scaled to the alloy composition. These represent the ideal model with no ordering, for the $Si_{0.5}Ge_{0.5}(001)$ dimer surface. The structure factors were subtracted from the measured structure factors for the $Si_{0.5}Ge_{0.5}$ film and then Fourier transformed. The result, shown in Fig. 8, clearly shows the compositional ordering to eight layers of the film. The positive densities in layers 3, 4, 7, and 8 correspond to the same locations of higher Ge composition in the refined model. Correspondingly, the negative contours around the opposite lattice site are locations of higher Si composition. Another result is the dipole density pattern at the dimer at-

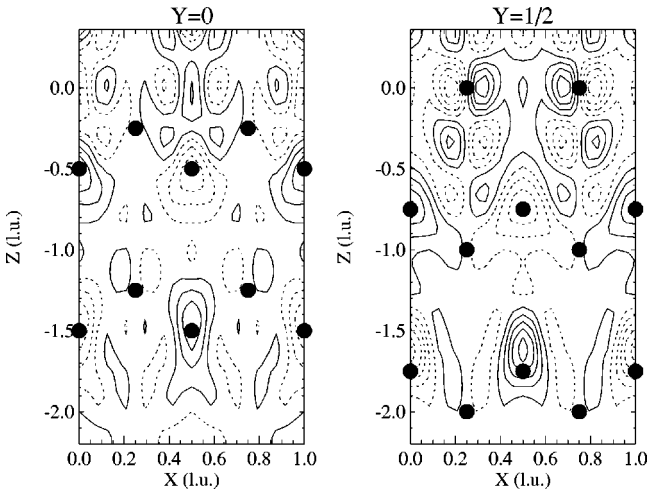

FIG. 8. Electron difference density map between $Si_{0.5}Ge_{0.5}$ and Ge(001) scaled to the same alloy density. The maps of the $y=0$ plane and of the $y=\frac{1}{2}$ plane show their atoms respective ideal (unreconstructed) positions as the solid circles. The contour lines are on the same scale as Fig. 7.

oms. This may represent an additional displacement of the dimer atoms, meaning the dimer length bond has shortened from that for the Ge(001). This conclusion is at variance with that of the refinement model above, but agrees with the points discussed above about the average SiGe lattice being smaller than Ge. As with the Ge(001) density maps, the reciprocal space cutoff to the data introduces meaningless minor peaks (oscillations) in areas between true atom positions, which can be ignored.

D. Thicker alloy films and their degree of order

In addition to the thinnest films analyzed above, a series of thicker $Si_{0.5}Ge_{0.5}$(001) films were grown on Ge(001) substrates. As expected, the amplitude of the compositional order peaks increases with film thickness. Figure 9 shows one set of the same surface reconstruction rod, the $(\frac{1}{2}1L)$, for four films, in order of increasing thickness. For the thickest film of 1000 Å, the ordering results in Bragg-like peaks at the $(\frac{1}{2},\frac{1}{2},\frac{1}{2})$ type position. The peaks at half order positions also have the characteristic alternation pattern of relative amplitudes, which confirm the RS2 structure found by Tischler *et al.*:[9] for the $(\frac{1}{2},1,L)$ data (shown in Fig. 9), the $L=0.5$ peak is expected to be the weaker peak, while the $L=1.5$ is stronger.

Our measurements are compared with the pure Ge(001) structure factors, also shown in Fig. 9. The Ge(001) structure factors provide an absolute scale with which to measure the alloy's structure factors, which can then be used to establish an absolute film order parameter. The calculation requires estimating the surface scattering component of the rods, shown in Fig. 9 as the intensity between the ordering peaks. This surface component is then subtracted from the specific values at the respective positions $L=0.5$ and 1.5. This overlap effect is important for the thinnest film of 30 Å, where the two sources of the scattering [the surface (2×1) reconstruction and the subsurface film ordering] have nearly the same magnitude. This has a profound effect on this rod at

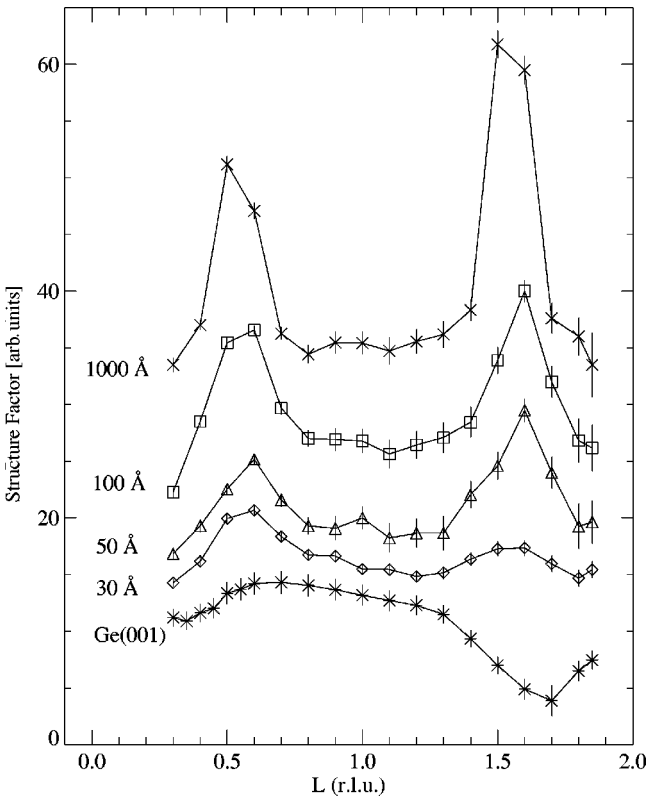

FIG. 9. Structure factor amplitude of the $(\frac{1}{2},1,L)$ rod from $Si_{0.5}Ge_{0.5}$ samples of various film thicknesses. Each curve is displaced from the next by $+5$ with the exception of the topmost one at $+15$. The alloy film thickness increases from 30 Å, 50 Å, 100 Å, and to 1000 Å. The bottom curve is the result of the same measurement for the pure Ge(001) (2×1) surface.

$L=1.5$, where the minimum in the surface diffraction signal becomes filled in by the $Si_{0.5}Ge_{0.5}$ ordering peak. This subtracting of structure factor components is an approximation that does not include the possible interference between the surface and film scattering components.

Once the absolute structure factor for the film's compositional ordering was determined, the film's thickness and the intrinsic RS2 scattering factors were used to normalize the values to give the films average order parameter in Table III. We used the square root of the thickness for the structure

TABLE III. Average film order parameters of $Si_{0.5}Ge_{0.5}$(001) for various film thickness and similar growth temperatures. Also listed are the determined ordering compositions of the (111) bilayers. The 8 ML thin film modeled above is the last entry (*) where the order parameter is the average from the resolved layers 3, 4, 7, and 8. The other entry for the 8 ML film is the result using the same method as for the other films.

Thickness	Growth Temp.	Order parameter, p	Ge%-Si%
1000 Å	450 °C	0.35 ± 0.09	68%
100 Å	475 °C	0.68 ± 0.03	84%
50 Å	400 °C	0.71 ± 0.07	86%
30 Å	450 °C	0.65 ± 0.05	83%
(8 ML) 10 Å	400 °C	0.21 ± 0.05	61%
(8 ML) 10* Å	400 °C	0.25 ± 0.02	63%

factors because the integrated intensity should be proportional to the thickness.[30] The values represent an average throughout the thickness of the film, rather than the specific ordering within individual domains. Table III also lists the film thickness and growth temperature. For the thinnest film, the average order parameter is also calculated from the least-squares fit from the occupancies of layers 3, 4, 7, and 8, assuming the other unresolved layers (5 and 6) have the same average ordering as those measured. The close agreement between the full model and the calculation method for thicker films validates the calculation method for the order parameter from the absolute structure factors.

An interesting result from this table is the increased ordering within the middle thicknesses of the $Si_{0.5}Ge_{0.5}$ thin films. The very thinnest film shows the smallest average order parameter. The thickest film at 1000 Å has the next smallest average order parameter. But in Fig. 9, this is the film with the largest absolute structure factor because of the film's bulk thickness. It is possible that the ordering is underestimated because of x-ray absorption in such a thick film. The other films have peaks that are lower in magnitude, and so the subtraction of the surface rod component is a larger factor in the results in Table III. This method of subtracting the surface rod component based on the Ge(001) structure factors may underestimate the full surface component, which can account for a large difference in order parameters between the fully modeled 8 ML film and the 30 Å film. It is satisfying that the largest order parameter is not above the physical limit of 1.0. Ordering parameters as high as 0.64 have been reported by other groups.[31,14]

The results in Table III do imply increased ordering where the film's morphology is changing: from fully strained, pseudomorphic growth at the least thickness, to the relaxed equilibrium $Si_{0.5}Ge_{0.5}$ lattice with misfit dislocations at the thickest film's interface. This result agrees with the proposed model by Jesson *et al.* for the ordering mechanism.[11] Their model suggests that both the increased step density and formation of 3D islands from strain relaxation are needed to form the long range order domains. This is inconsistent with our result for the thinnest films, which are assumed to be pseudomorphic and fully strained, however. This point has been presented before in Ref. 31, which reports continued compositional ordering in films grown on graded buffer layers to the composition of 60% Ge on the Si(001) substrate. The graded buffer layers provided a flat, strain-relieved growth surface, not the strained and island morphology supposedly required by Jesson *et al.*

As part of this experiment, several of the thicker films were also examined by scanning tunneling microscopy (STM) in another UHV analysis chamber attached to the same vacuum transfer system.[32] The surface morphologies showed a total lack of one important feature assumed in both models for the compositional ordering mechanism: double height steps, or at least single steps in close proximity. The STM measurements where done immediately after the samples were cooled from MBE growth temperature at a quench rate of approximately 2 °C/min. Both models rely on a growth morphology with double height steps in order for the growth of successive layers to have the same orientation of their 2×1 dimer rows. Conversely, single step flow growth leads to each successive layer having the dimer rows rotated 90°, as we observed by STM. This means that, for either proposed ordering mechanism, each successive layer must order along another 111 plane, 90° from the previous layers. This process cannot result in the observed domain structure of compositional order, with each domain ordered along a unique 111 direction.[9,31,33] Our observation of only single height steps on the surface of the ordering SiGe alloy films is a significant point that is difficult to explain by minor modifications of either of the proposed growth mechanisms.

IV. CONCLUSION

Our experiments using surface x-ray diffraction have revealed details of the compositional ordering that occurs during the growth of thin films of $Si_{1-x}Ge_x(001)$. For the thinnest film of 8 ML (10 Å), the atomic order parameter and the Fourier difference map analysis both showed the migration of Ge atoms to the tensile strained sites and Si atoms to the compressive strained sites beneath the surface (2×1) dimer reconstruction. Farther below the surface the compositional ordering was present in the lattice sites consistent with the initial formation of the RS2 $Si_{0.5}Ge_{0.5}$ structure and its bilayer (111) planes. Although our experiment could not resolve any possible ordering in the symmetric sites below the dimer surface (layers 5 and 6), the results were consistent with the crystallographic experiment by Tischler *et al.* and their results for the RS2 structure.[9] The ordering along the (111) planes must continue through layers 5 and 6, but the equal distribution of ordering domain across the film obscured this in our experiment.

The Fourier difference map of our $Si_{0.5}Ge_{0.5}$ structure factors also provided evidence for compositional ordering by direct comparison with the Ge(001) dimer reconstructed surface. Unlike model refinement, this method is a direct calculation, independent of any bias, except from the phases calculated from the model of Ge(001).[18] Besides the compositional ordering in the layer beneath the dimer, the difference map showed an additional displacement of the dimer atoms to a shorter bond length. This is an opposite conclusion to the refinement model, which found an increased dimer bond length. This disagreement may be related to uncertainty in roughness parameters used in both procedures. The surface roughness, which decreases the coherence of the surface diffraction, is implicit within the overall scale factor for the refinement model, and within the scale factor used to scale the Ge(001) data to the same average compositional density as the $Si_{0.5}Ge_{0.5}$. Each of these parameters was refined independently.

The measurements from thicker films of $Si_{0.5}Ge_{0.5}(001)$ provided information on how the strength of the order parameter changes with film thickness. The ordering was found to increase with film thickness up to a maximum at the thickness of about 50–100 Å. Here, the order was 2.5–3 times the amount found in the initial stages of growth (i.e., the 8 ML film discussed above). The degree of compositional order then decreased again for our thickest sample (1000 Å). The thin-film portion of this thickness trend might be explained by effects of the internal interface between the alloy film and its substrate. If the interface tends to suppress the chemical

order, this will be reflected as a reduced order parameter in the thinnest films, which can be approximated by an effective number of ''dead layers.'' The data of Table III (except those for the thickest sample) would be consistent with approximately 7 Å of each film not contributing and a saturation order parameter of 0.8.

The surface x-ray diffraction experiment has identified features that agree with both proposed mechanisms for the origin of compositional ordering within $Si_{0.5}Ge_{0.5}(001)$ films. The clearest result is the chemical ordering observed in the subsurface layers under the dimer reconstruction from the experiment on the thinnest film. This confirms the predictions by Kelires and Tersoff,[16] which are the basis for the model mechanism by LeGoues *et al.*[13]

ACKNOWLEDGMENTS

We acknowledge the support for this work from the U.S. Department of Energy under Contract No. DEFG02-96ER45439 to the Materials Research Laboratory. K.L.W. acknowledges support from the U.S. Department of Education under Contract No. DE-P200-A40532. Part of this work was carried out in the Center for Microanalysis at the Materials Research Laboratory.

*Present address: Rockwell Science Center, 1049 Camino Dos Rios, Thousand Oaks, CA 91360.

†Present address: Wright Laboratory, Bldg. 620, 2241 Avionics Circle, Wright-Patterson Air Force Base, OH 45433.

[1] A. Ourmazd and J.C. Bean, Phys. Rev. Lett. **55**, 765 (1985).

[2] D.J. Lockwood, K. Rajan, E.W. Fenton, J.M. Baribeau, and M.W. Denhoff, Solid State Commun. **61**, 465 (1987).

[3] E. Müller, H.U. Nissen, M. Ospelt, and H. von Känel, Phys. Rev. Lett. **63**, 1819 (1989).

[4] José Luís Martins and Alex Zunger, Phys. Rev. Lett. **56**, 1400 (1986).

[5] M. Hansen, *Constitution of Binary Alloys*, 2nd ed. (McGraw-Hill, New York, 1958).

[6] P. B. Littlewood, Phys. Rev. B **34**, 1363 (1986).

[7] B. Koiller and M. O. Robbins, Phys. Rev. B **40**, 12 554 (1989).

[8] D.E. Jesson, S.J. Pennycook, and J.M. Baribeau, Phys. Rev. Lett. **66**, 750 (1991).

[9] J.Z. Tischler, J.D. Budai, D.E. Jesson, G. Eres, P. Zschack, J.M. Baribeau and D.C. Houghton, Phys. Rev. B **51**, 10 947 (1995).

[10] F.K. LeGoues, R.M. Tromp, V.P. Kesan, and J. Tsang, Phys. Rev. B **47**, 10 012 (1993).

[11] D.E. Jesson, S.J. Pennycook, J.-M. Baribeau, and D.C. Houghton, Phys. Rev. Lett. **68**, 2062 (1992).

[12] T. Araki, N. Fujimura, T. Ito, A. Wakahara, and A. Sasaki, J. Appl. Phys. **80**, 3804 (1996).

[13] F.K. LeGoues, V.P. Kesan, S.S. Iyer, J. Tersoff, and R.M. Tromp, Phys. Rev. Lett. **64**, 2038 (1990); V.P. Kesan, F.K. LeGoues, and S.S. Iyer, Phys. Rev. B **46**, 1576 (1992).

[14] J.C. Tsang, V.P. Kesan, J.L. Freeouf, F.K. LeGoues, and S.S. Iyer, Phys. Rev. B **46**, 6907 (1992).

[15] D.E. Jesson, S.J. Pennycook, J.Z. Tischler, J.D. Budai, J.M. Baribeau, and D.C. Houghton, Phys. Rev. Lett. **70**, 2293 (1993).

[16] P.C. Kelires and J. Tersoff, Phys. Rev. Lett. **63**, 1164 (1989).

[17] R. Rossman, H. L. Meyerheim, V. Jahns, J. Wever, W. Moritz, D. Wolf, D. Dornisch, and H. Schulz, Surf. Sci. **279**, 199 (1992).

[18] X. Torrelles, H.A. van der Vegt, V.H. Etgens, P. Fajardo, J. Alvarez, and S. Ferrer, Surf. Sci. **364**, 242 (1996).

[19] M. Takahashi, S. Nakatani, Y. Ito, T. Takahashi, X.W. Zhang, and M. Ando, Surf. Sci. Lett. **338**, L846 (1995).

[20] R. Felici, I. K. Robinson, C. Ottaviani, P. Imperatori, P. Eng, and P. Perfetti, Surf. Sci. **375**, 55 (1997).

[21] B.E. Warren, *X-ray Diffraction* (Addison-Wesley, Reading, MA, 1969).

[22] H. Reichert, P.J. Eng, H. Dosch, and I.K. Robinson, Phys. Rev. Lett. **74**, 2006 (1995); A.P. Baddorf and S.S. Chandavarkar, Physica B **221**, 141 (1996).

[23] I.K. Robinson and D.J. Tweet, Rep. Prog. Phys. **55**, 599 (1992).

[24] X.J. Zhang, G. Xue, A. Agarwal, R. Tsu, M.-A. Hasan, J.E. Greene, and A. Rockett, J. Vac. Sci. Technol. A **11**, 2553 (1993).

[25] J.E. Van Nostrand, Ph.D. thesis, University of Illinois at Urbana-Champaign (1996).

[26] J.E. Van Nostrand, S. J. Chey, M.-A. Hasan, D.G. Cahill, and J.E. Greene, Phys. Rev. Lett. **74**, 1127 (1995).

[27] K.L. Whiteaker, Ph.D. thesis, University of Illinois at Urbana-Champaign (1997).

[28] I. K. Robinson, in *Handbook on Synchrotron Radiation*, Vol. 3, edited by G. Brown and D. E. Moncton (Elsevier, Amsterdam, 1991), Chap. 7.

[29] S. Ferrer, X. Torrelles, V.H. Etgens, H.A. van der Vegt, and P. Fajardo, Phys. Rev. Lett. **75**, 1771 (1995).

[30] For a discussion of the bulk integrated intensity and structural order parameter determination, see B. E. Warren, *X-ray Diffraction* (Addison-Wesley, Reading, MA, 1969).

[31] F.K. LeGoues, J. Tersoff, and R.M. Tromp, Phys. Rev. Lett. **71**, 3736 (1993).

[32] J.E. Van Nostrand, D.G. Cahill, I. Petrov, and J.E. Greene, J. Appl. Phys. (to be published).

[33] F.K. LeGoues, V.P. Kesan, and S.S. Iyer, Phys. Rev. Lett. **64**, 40 (1990).